КОМПЬЮТЕРНЫЕ ТЕХНОЛОГИИ В ФИЗИКЕ

GEANT4 SIMULATION OF dp NONMESONIC BREAKUP REACTION AT 300 AND 500 MeV

M. Janek [a,1], *B. Trpišová* [a], *S. M. Piyadin* [b], *V. P. Ladygin* [b]

[a] Physics Department, University of Žilina, Žilina, Slovakia

[b] Joint Institute for Nuclear Research, Dubna

GEANT4 simulations of the reaction $dp \to ppn$, i.e., the dp nonmesonic breakup reaction, at 300 and 500 MeV of deuteron energy for different detector configurations are presented. Two threads made from polyethylene and carbon with a thickness of 10 μm are used as targets. The goal of the simulations is to find a method by means of which the signal from the dp nonmesonic breakup can be separated from the background that mainly comes from the carbon content of the CH_2 target. The obtained results will be used in the experimental spin program that will be realized at the Nuclotron in Dubna. The aim of this experimental investigation is to contribute to the elucidation of the structure of the spin-dependent parts of the nucleon–nucleon and three-nucleon forces acting in the dp nonmesonic breakup. The deuteron energies will be ranging from 300 up to 500 MeV.

Представлены результаты GEANT4 моделирования для реакции $dp \to ppn$, т. е. реакции dp безмезонного развала, при энергии 300 и 500 МэВ для различных кинематических конфигураций. В качестве мишеней используются две нитки толщиной 10 мкм, изготовленные из полиэтилена и углерода. Целью моделирования является поиск метода, с помощью которого сигнал от dp безмезонного развала может быть отделен от фона, который, в основном, происходит от вклада углерода в CH_2-мишени. Полученные результаты будут использованы в экспериментальной спиновой программе, которая реализуется на нуклотроне в Дубне. Целью экспериментального исследования является вклад в изучение структуры спин-зависимых частей нуклон-нуклонных и трехнуклонных сил, действующих в реакции безмезонного развала дейтрона. Энергии дейтрона находятся в пределах от 300 до 500 МэВ.

PACS: 21.45.-v; 24.10.Lx; 25.10.+s

INTRODUCTION

Intensive theoretical and experimental investigation of short-range nucleon correlations has been conducted in the past years. The dominant contribution of the nucleon–nucleon (NN) short-range correlations was pointed out by the experiments performed at BNL [1], SLAC [2] and JLAB [3, 4] in which 90% of all nucleons with internal momenta $k > 300$ MeV/c belonged to the NN short-range correlations. At the same time, the three-nucleon ($3N$) short-range correlations for the same range of k's exhibited also a significant probability [5] confirming the importance of including the three-nucleon forces (3NFs) in the theory.

In case of the $dp \to ppn$ reaction, i.e., the dp nonmesonic breakup reaction (in the following text just «the dp breakup»), the short-range nucleon correlations are represented

---

[1] E-mail: janek@jinr.ru

mainly by the *NN* potentials and the 3NFs. This reaction is one of the simplest ones in which the structure of these objects can be studied. Below we select some results obtained over the past years for nuclear reactions involving nucleons or deuterons and nucleons to illustrate the current status of this subject.

Deuterons and nucleons can be considered to be few-body systems for the description of which the nonrelativistic Schrödinger equation that includes only the *NN* potentials as a starting point can be used. This is possible because of the relative smallness of the typical energies involved in the nuclear reactions in which these particles take part. It has been shown that the data obtained from the *NN* scattering at low and intermediate energies can be described with high precision using the *NN* potentials only (e.g., CD-Bonn [6]). These modern *NN* potentials, however, underestimate the binding energies of the three-nucleon systems ^{3}H and ^{3}He by about 0.5–1 MeV [7] and do not reproduce the *dp* breakup and *dp* elastic scattering data.

The investigation of the *nd* scattering at energies below 30 MeV has revealed that the cross sections and the tensor analyzing powers obtained on the basis of experimental data are rather well described with the corresponding theoretical calculations in which only the *NN* potentials have been used. In case of the vector analyzing power A_y, such an agreement could not be achieved using any known *NN* potential. The inclusion of the 3NFs did not improve the situation either, leading to the well-known A_y puzzle. It has also been demonstrated that the cross-section data of the *pd* elastic scattering obtained at 250 MeV cannot be reproduced by the Faddeev calculations [8]. The reason for these discrepancies may be the possible existence of a new type of short-range 3NFs that, for obvious reason, could not be included in the calculations. On the other hand, it has been found that in the vicinity of the Sagara discrepancy the currently known 3NFs contribute by up to 30% to the *dp* elastic scattering cross section at intermediate energies [9, 10].

The *dp* breakup possesses rich kinematics or phase space. The effects originating from the 3NFs dominate in some regions of the phase space, the relativistic effects in other ones. The Coulomb effects can be investigated in regions of the phase space where the 3NFs and relativistic effects are weak. Thus, to obtain data for a large region of the phase space, it is desirable to get complementary information about the reaction mechanism and the structure of the objects involved in the *dp* breakup. Using the *pd*-breakup data collected at 19 MeV [11], a discrepancy between the data and the calculations that included the 3NFs has been found. Inclusion of the Coulomb interaction is very significant but in this case did not completely remove discrepancy. Large discrepancies between experiment and theoretical calculations based on various *NN* and 3*N* potentials have also been found in case of the *dp* breakup measured at 130 MeV [12]. It has been shown, however, that theoretical calculations based on low energy expansion of QCD, i.e., the Chiral Perturbation Theory (χPT), can satisfactorily describe data obtained for energies up to 100 MeV/nucleon.

To summarize, the currently known *NN* and *3N* potentials are in many cases in good agreement with experiment, but in some cases they are not. Thus, it is necessary to look for new types of these potentials or even for potentials involving more than three nucleons.

1. DETECTOR SETUP

In the experiments carried out at the Nuclotron in Dubna, the *dp* breakup has been detected by the simultaneous registration of two protons by two detectors — the two detectors work in coincidence. The energies of the deuterons will be ranging from 300 to 500 MeV.

Eight $\Delta E - E$ detectors will be used. Each detector consists of two scintillators, thin — ΔE, and thick — E. Both scintillators are of a tube shape, the thin one of a height of 1 cm, the thick one of a 20 cm height, with the diameter of the cross section 8 and 10 cm, respectively. Two photomultiplier tubes PMTs-85 will be positioned opposite to each other at the outside cylindrical surface of the thin scintillator as shown in Fig. 1. The ΔE scintillator surface has been polished in order to increase the area of the optical contact between the scintillator and the photocathode of the PMT-85. This scintillator is covered by white paper, and digital dividers of high voltage will be used for the PMT-85.
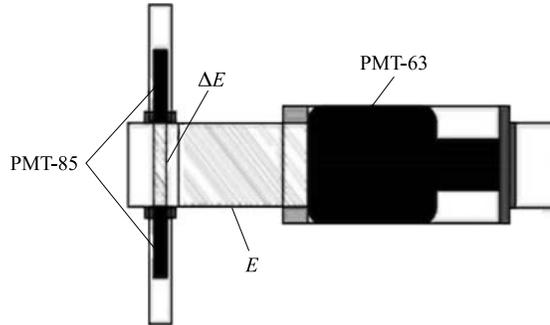

Fig. 1. Sketched view of $\Delta E - E$ detector

At the bottom end of the E scintillator a photomultiplier tube PMT-63 will be positioned. The E scintillator is also covered by white paper. The contact area of the two scintillators is covered by black paper in order to exclude the possibility of light transfer between them. The details of the $\Delta E - E$ detector construction can be found in [13].

Each detector will be positioned at a distance of 99.6 cm from the target so that the angle whose vertex is the target subtended by the diameter of the thin scintillator is $4.6°$. As mentioned above, the target will have a shape of a thin thread of thickness $10\,\mu$m. It will be enclosed in a spherical hull made from stainless steel with an external diameter of 160 mm and a thickness of 0.5 mm. There are two openings on the opposite sides of the hull to let pass the bunches of deuterons that are being accelerated along a circular path. After reaching the required energy the mechanism connected with the hull ejects the target so that it intersects the trajectory of the deuteron beam.

To produce collisions of the deuteron with hydrogen, polyethylene (CH_2) targets will be used since targets made from pure hydrogen are expensive and they would produce a very small statistics. On the other hand, when the CH_2 target is bombarded with deuterons, large background is present. Furthermore, the Nuclotron detectors detect only charged particles without specifying their type. Hence, ways must be found for selecting our signal events out of all detected events and this should be done for various detector configurations. To accomplish this goal, we have performed computer modeling using the GEANT4 toolkit [14].

2. SIMULATION

As stated above, we simulated the collision of the deuteron beam with protons (the hydrogen) using a CH_2 target. We found that when bombarding the CH_2 target with deuterons in the vast majority of cases the two detectors detect in one event two protons and very rarely

other particles or more than two particles obviously mostly from the collisions of the deuterons with the carbon nuclei. One also has to realize that some fraction of the two proton events will not represent the *dp* breakup but will also come from the collisions of the deuteron with the carbon nuclei. As will be discussed below, the events represented by the collisions of deuterons with the carbon nuclei form the *dp* breakup background that we simulated by the collisions of the deuterons with a carbon target, i.e., by the *d*C events. Then by subtracting the *d*C events from the *d*CH$_2$ events, the signal events can be selected.

Due to the lower performance of the available computers, we performed the simulation in two steps. This was possible because of the polar symmetry of the reaction. In the first step, a deuteron beam of required energy hits the target. The types of the outgoing particles, their energy and their scattering angle, i.e., the angle made by the trajectory of the outgoing particle and the direction of the deuteron beam, are recorded only if this angle is greater than $17°$. The reason for this cut is that roughly for scattering angles smaller than $17°$ the collisions of the deuterons with the CH$_2$ target produce large background that is mainly due to the carbon content of the target.

In order to realize the second step, we put two $\Delta E{-}E$ detectors at a distance of 99.6 cm from the target in such a way that their longitudinal axes pass through the target and make angles that we designated Θ_1 and Θ_2 with the trajectory of the incoming deuterons. The angle between detectors in plane perpendicular to the direction of the deuteron beam is denoted by Φ. The three angles Φ, Θ_1 and Θ_2 specify a detector configuration. The configurations for which we present our results are given in table. As one can notice, the angles Θ_1 and Θ_2 appear as an interval of angles, which is due to the finite size of the detectors' cross section.

Detector configurations description

Configuration	Θ_1, deg	Θ_2, deg	Φ, deg
2	22.4–27.0	31.0–35.6	40
5	22.4–27.0	40.9–45.5	180
19	31.0–35.6	40.9–45.5	130
23	40.9–45.5	40.9–45.5	180
28	51.0–55.6	51.0–55.6	180

Then we shot the particles generated in the first step at the recorded angles from the center of the target. To analyze our data, we calculated the invariant mass distribution of two charged particles (in the following text just the invariant mass) that hit the detectors in one event. We used as the particles' kinetic energy (incoming energy) the energy they deposited in the detectors and the mean value of the range of angles Θ_1 and Θ_2 for the relevant detector configuration as the directions of the particles momenta. GEANT4 gives these directions exactly as the scattering angles of the particles, but we must simulate conditions provided in the experiment in which this information will not be available.

One of the assumptions for obtaining undistorted results in determining the invariant mass is to use the correct value of the particles' incoming kinetic energy. The selection of the correct events was done by means of $\Delta E{-}E$ energy correlation plots and further modeling. The $\Delta E{-}E$ energy correlation plots are graphs showing the correlation of the energies deposited in the ΔE and E detectors that we named ΔE and E, respectively. Such a plot generated for the CH$_2$ target bombarded with 500 MeV deuterons for the detector

configuration 2 is depicted in Fig. 2. The area surrounded by the red curve, designated as cut1, includes events in which the detected particles pass through the detector basically along its longitudinal direction and stay in it; i.e., they deposit there all of their kinetic energy. The part of the plot surrounded by the blue curve, designated as cut2, contains events in which the detected particles pass through the detector basically along its longitudinal direction but after depositing some part of their kinetic energy there leave it. Hence, the calculation of the invariant mass for these particles does not give its correct value, either, which means that these events should also contribute to the background in the invariant mass spectra. It will be shown below, however, that a part of this background are actually our signal events.
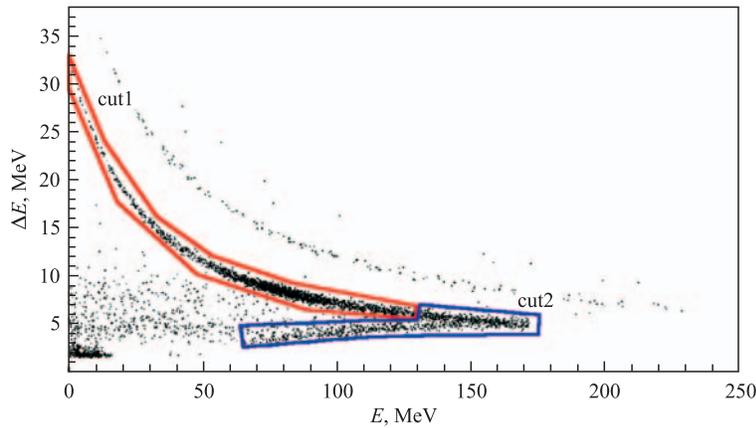

Fig. 2 (color online). Correlation of energies deposited in the ΔE and E detectors. The selection of events surrounded by the red curve is named cut1 and the selection of events surrounded by the blue curve is named cut2. The calculation was done for the CH_2 target, 500 MeV deuterons and the detector configuration 2

Another contribution to the background is constituted by the events in which the particles registered by the detectors are not protons since in the calculation of the invariant mass we assume that two protons are detected; i.e., we use the rest mass of protons in the invariant mass formula. The main part of the background in the invariant mass plots is due to the protons that come from the collision of the deuteron with the carbon nuclei. As discussed above, the background can be removed by the subtraction of the dC spectra from the dCH$_2$ spectra.

In Fig. 2 the area that corresponds to the cut2 events contains events for which the incoming energies of the particles are greater than about 180 MeV. We arrived at this result by plotting the deposited energy versus the incoming energy. The importance of it will become clear when discussing Figs. 3 and 4, which depict the invariant mass distribution of the two charged particles registered by the detectors when the deuteron energy is 300 and 500 MeV, respectively.

In Figs. 3 and 4 we present invariant mass distributions calculated for 300 and 500 MeV deuterons. The non-shaded spectra represent the dCH$_2$ simulations and the shaded ones the dC simulations. The dC spectra are normalized against the dCH$_2$ spectra according to the regions where only the carbon content is expected. Each of these figures contains six plots arranged in three rows and two columns. The rows correspond to the detector configurations
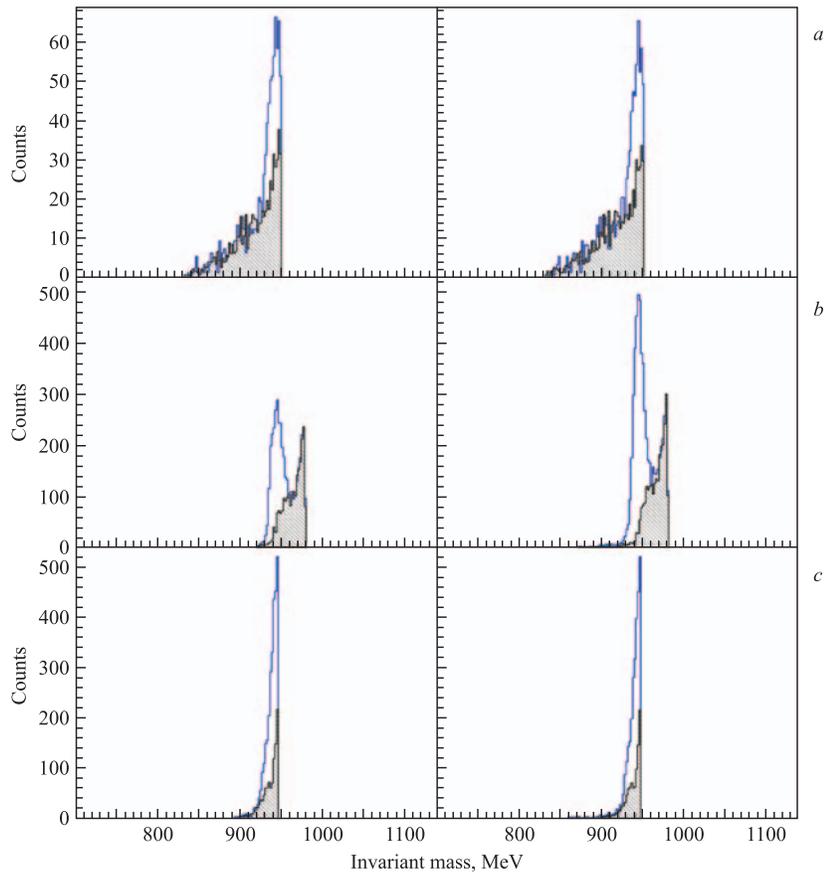
Fig. 3. Invariant mass distribution obtained for CH_2 (non-shaded spectra) and carbon (shaded spectra) targets that were bombarded with deuterons of energy 300 MeV. The detector configurations are 2 (top row), 5 (middle row) and 19 (bottom row), respectively. Left (right) column corresponds to the cut1 (cut1 plus cut2) selection of events

2, 5 and 19 given in table, the first column represents the spectra calculated using the cut1 events, in the second column are depicted spectra calculated using both cut1 and cut2 events. The graphs in the figures exhibit clear peaks at about 940 MeV, i.e., at the value of the rest mass of neutron. Thus, in view of what we have said above about the background that we get in the calculated invariant mass spectra, the events corresponding to this peak are mostly our *dp*-breakup events and calculating the invariant mass is a good means of how to separate them from the rest of the events.

Examination of the plots in Fig. 3 shows that there are only small differences between the invariant mass distributions calculated using the cut1 and the cut1 plus cut2 selection of events except for the graphs corresponding to configuration 5 (Fig. 3, *b*). This is due to the fact that for the deuteron energy 300 MeV only a small fraction of scattered particles has energy larger than about 180 MeV.
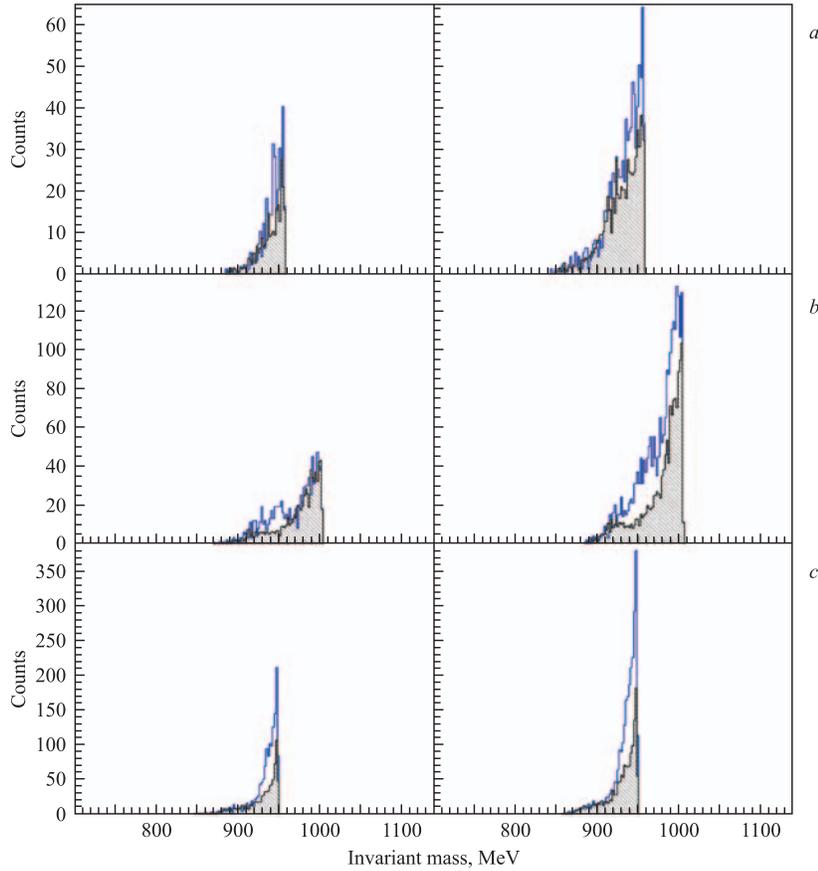
Fig. 4. Invariant mass distribution for CH_2 (non-shaded spectra) and carbon (shaded spectra) targets that were bombarded with deuterons of energy 500 MeV. The detector configurations are 2 (top row), 5 (middle row) and 19 (bottom row), respectively. Left (right) column corresponds to the cut1 (cut1 plus cut2) selection of events

On the other hand, using the cut1 and cut1 plus cut2 selection of events in case of the 500 MeV deuterons made it possible to localize in the calculated invariant mass spectra those events in which the energy of the incoming protons is larger than about 180 MeV. We found that these events are shifted towards the right part of the spectra as mainly Fig. 4, *b* demonstrates. Since GEANT4 gives the incoming energies of the particles, we could calculate the invariant mass for these events with the correct value of their kinetic energy (that should be ideally whole deposited in the detectors) and we found that these events are also the *dp*-breakup events, i.e., the signal events. In case of the 500 MeV deuterons, especially marked is the cut1 effect on the signal when a large part of it is cut out.

The main reason of the peak spreading in the invariant mass spectra depicted in Figs. 3 and 4 and of the shifting to the right in case of the cut1 plus cut2 selection of events in the 500 MeV deuterons spectra is connected with using of mean angle of the detector in calculation. In this way we simulate the real experimental conditions at which the scattering

angles of the detected particles will not be known. Other reasons of the peak spreading are associated with the detector response. We also modelled the effect of the spherical steel hull on energy and direction of motion of the particles going out of the target. We found that the hull affects the scattering angles and causes considerable energy losses for particles of only very low energies (roughly of energies smaller than 35 MeV) and these are cut out by the $\Delta E - E$ coincidence condition, that means, they stop already in the thin scintillator and thus the events involving such particles are not counted as events.

Hence, we conclude that two methods of reconstructing the signal events are possible. The first one is calculating the dCH$_2$ and dC spectra using only the cut1 selection of events and subsequently applying the above-described subtraction procedure. The second one is based on the localization of the dp-breakup events by means of the GEANT4 simulation that uses both cut1 and cut2 selections of events with the subsequent subtraction of the dC spectra from the dCH$_2$ spectra. The pictures in the top row in Fig. 4 also show that for these cases the yield is low or negligible. Thus, we see that the subtraction procedure can be used for selecting the signal events in the invariant mass spectra, but the yield varies with the energy of the incoming deuterons and the detector configuration.

In Fig. 5 we present a comparison of the experimental data obtained in the Nuclotron run realized in 2012 (non-shaded) and our simulations (shaded). The spectra correspond to configurations 23 (Fig. 5, a) and 28 (Fig. 5, b) and 500 MeV deuterons. An experimental study of the $dp \rightarrow ppn$ reaction at the deuteron energy of 500 MeV that took place at the Nuclotron
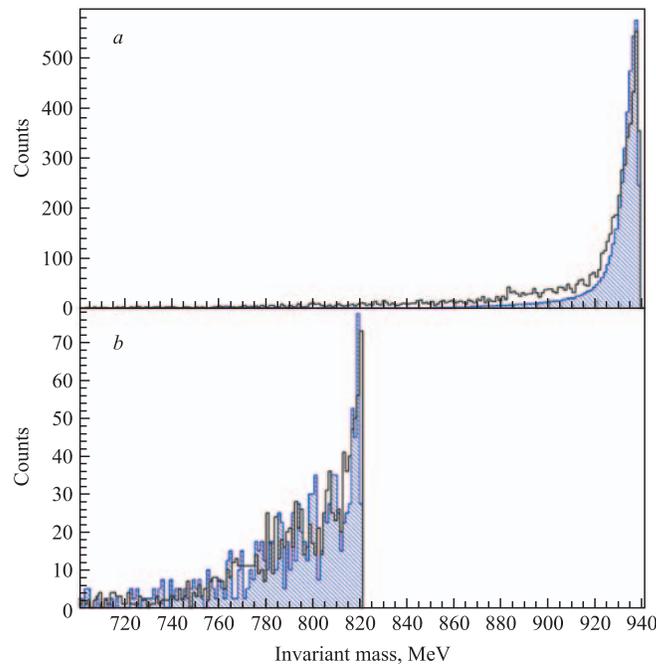

Fig. 5. Simulated (shaded) and experimental (non-shaded) plots of the invariant mass distribution obtained using the CH$_2$ target for the detector configurations 23 (a) and 28 (b) (see table). The deuteron energy is 500 MeV. In both the simulated and the experimental spectra the cuts are $\Delta E > 0$ MeV and $E > 0$ MeV

under a different detector configuration than that used in the 2012 Nuclotron run was described in [15]. Compared to the cut1 and cut2 cuts, both the experimental and the simulated invariant mass distributions were obtained under the conditions $\Delta E > 0$ MeV and $E > 0$ MeV to cut out unphysical events to which usually zero or negative energies are assigned. We note that using cut1 and cut2 selection of events removes such events automatically, as our invariant mass spectra presented in Figs. 3 and 4 demonstrate. The spectra in Fig. 5 are scaled; i.e., we multiplied the simulated spectra by a constant in order to make the comparison of the experimental data with the simulated data easier. As can be seen, the simulated invariant mass distributions and the experimental ones are in good agreement.

Some discrepancy between the simulated and the experimental data can be caused by the deuteron beam parameters. Another possible source of this discrepancy can be connected with the models GEANT4 used in the simulation of the collisions of the deuterons with the CH_2 target. To simulate hadronic interactions, GEANT4 uses the QBBC physics list which contains the Binary Cascade model.

CONCLUSIONS

We present results of the GEANT4 simulations of the $dp \rightarrow ppn$ reaction — the dp nonmesonic breakup reaction — at deuteron energies of 300 and 500 MeV for various configurations of two $\Delta E - E$ detectors that will be used in experiments planned at the Nuclotron in Dubna.

To simulate the signal events, we used a CH_2 target. We recorded only events in which the scattering angles of the outgoing particles are larger than $17°$ since for smaller scattering angles there occurs a large background.

To separate the signal from the background, we calculated the invariant mass distributions of two charged particles, assuming that these two particles are protons. Then the signal events should form a peak centered at an energy of about 940 MeV — the rest mass of neutron — and our results confirmed this expectation. The rest of the events form the background of the invariant mass spectra that can be largerly removed by means of the subtraction procedure.

The second part of the background in the invariant mass spectra is constituted by the signal events in which the protons pass through the detector and leave it, depositing only a part of their kinetic energy there, which results in incorrect values of the invariant mass. By means of our modeling using the GEANT4 software, however, we could localize these events in the spectra. The modeling also revealed that these particles possess kinetic energies greater than 180 MeV.

When calculating the invariant mass, we used two different selection of events that we called cut1 and cut2. Only when comparing the simulated data with the experimental ones, we used a different cut. The selection cut1 contains mainly events in which the particles hitting the detectors stop in them; the selection cut2 represents events in which the outgoing particles pass through the detectors, depositing only a part of their kinetic energy there. By such means we could find those signal events which produce incorrect values of the invariant mass, since only a part of the kinetic energy of the particles taking part in these events is deposited in the detectors.

As can be deduced from the considerations given in the previous section, the kinetic energy of the particles going out of the target increases with the increasing energy of the

deuterons. The invariant mass distributions calculated in case of the 300 MeV deuterons mostly do not contain incorrect invariant mass values of the *dp*-breakup events, since all of the kinetic energy of the detected protons is deposited in the detectors. In case of the 500 MeV deuterons, in a large number of events only a part of the kinetic energy of the protons is deposited in the detectors, thus producing incorrect values of their invariant mass. Such events can be removed by using only the cut1 selection of events, but doing so also signal events are cut out. However, one can select all signal events, that means also those that do not exhibit the correct values of the invariant mass and applying the subtraction procedure taking into account their location.

We note that the simulated invariant mass spectra are normalized according to those of their regions where only the events corresponding to the collisions of the deuterons with the carbon nuclei are located. However, the normalization is questionable if such a region is very narrow, which can be due to a large content of the misplaced *dp*-breakup events, i.e., the signal events with the incorrect value of the invariant mass.

To conclude, our GEANT4 modeling suggests that the subtraction of the dC from the dCH$_2$ invariant mass of two charged particles spectra may be a useful tool for separating the *dp*-breakup events from the rest of the events originating in the deuteron collisions with the CH$_2$ target. Further, as we have clearly demonstrated in this work, this modeling makes it possible to identify those signal events that are not located in the peak around 940 MeV due to the incorrect invariant mass values caused by only a partial deposition of the kinetic energy of the signal protons in the detectors. Clearly, such an identification cannot be done solely by an experiment. Of nonnegligible importance is also our GEANT4 modeling of the effect of the spherical steel hull that surrounds the target on the energies and scattering angles of the particles leaving the target. Hence, using the GEANT4 software may be very useful in preparing and analyzing the *dp*-breakup experiments running at the Nuclotron in Dubna.

REFERENCES

1. *Piasetzky E. et al.* Evidence for the Strong Dominance of Proton–Neutron Correlations in Nuclei // Phys. Rev. Lett. 2006. V. 97. P. 162504.

2. *Frankfurt L. L. et al.* Evidence for Short-Range Correlations from High Q^2 (e, e') Reactions // Phys. Rev. C. 1993. V. 48. P. 2451.

3. *Egiyan K. S. et al.* Observation of Nuclear Scaling in the A (e, e') Reaction at $x(B)$ Greater than 1 // Phys. Rev. C. 2003. V. 68. P. 014313.

4. *Egiyan K. S. et al.* Measurement of 2- and 3-Nucleon Short-Range Correlation Probabilities in Nuclei // Phys. Rev. Lett. 2006. V. 96. P. 082501.

5. *Machleidt R., Sammarruca F., Song Y.* The Nonlocal Nature of the Nuclear Force and Its Impact on Nuclear Structure // Phys. Rev. C. 1996. V. 53. P. 1483.

6. *Nogga A. et al.* Benchmark Calculations for the Triton Binding Energy for Modern *NN* Forces and the $\pi\pi$ Exchange Three-Nucleon Force // Phys. Lett. B. 1997. V. 409. P. 19.

7. *Hatanaka K. et al.* Cross-Section and Complete Set of Proton Spin Observables in p Polarized d Elastic Scattering at 250 MeV // Phys. Rev. C. 2002. V. 66. P. 044002.

8. *Sakamoto N. et al.* Measurement of the Vector and Tensor Analyzing Powers for the $d-p$ Elastic Scattering at $E_d = 270$ MeV // Phys. Lett. B. 1996. V. 367. P. 60.

9. *Sekiguchi K. et al.* Complete Set of Precise Deuteron Analyzing Powers at Intermediate Energies: Comparison with Modern Nuclear Force Predictions // Phys. Rev. C. 2002. V. 65. P. 034003.

10. *Ley J. et al.* Cross Sections and Tensor Analyzing Powers A_{yy} of the Reaction ^{1}H(*d, pp*)*n* in «Symmetric Constant Relative Energy» Geometries at $E_d = 19$ MeV // Phys. Rev. C. 2006. V. 73. P. 064001.

11. *Kistryn S. et al.* Evidence of Three-Nucleon Force Effects from 130-MeV Deuteron Proton Breakup Cross-Section Measurement // Phys. Rev. C. 2003. V. 68. P. 054004.

12. *Piyadin S. M. et al.* $\Delta E-E$ Detector for Proton Registration in Nonmesonic Deuteron Breakup at the Nuclotron Internal Target // Phys. Part. Nucl. Lett. 2011. V. 8, No. 2. P. 107.

13. *Agostinelli S. et al.* GEANT4 — a Simulation Toolkit // Nucl. Instr. Meth. A. 2003. V. 506, No. 3. P. 250.

14. *Piyadin S. M. et al.* The Study of the $dp \rightarrow ppn$ Reaction at the Internal Target Station at the Nuclotron at Deuteron Energy of 500 MeV. JINR Preprint P1-2013-13. Dubna, 2013.